Electronic Supplementary Material (ESI) for Chemical Communications.
This journal is © The Royal Society of Chemistry 2017

# Electronic Supplementary Information (ESI)

# LanthanoPlatins: Emissive Eu(III) and Tb(III) complexes staining nucleoli targeted through Pt-DNA crosslinking

Khushbu Singh,[a] Swati Singh,[b] Payal Srivastava,[a] Sri Sivakumar,[b] and Ashis K. Patra*[a]

[a]Department of Chemistry, Indian Institute of Technology Kanpur, Kanpur 208016, Uttar Pradesh, India.

[b]Department of Chemical Engineering and Centre for Environmental Science and Engineering, Indian Institute of Technology Kanpur, Kanpur 208016, Uttar Pradesh, India.

| | Table of contents | Page |
|---|---|---|
| **1** | **Experimental** | |
| 1.1 | Materials | **4** |
| 1.2 | Physical methods, photostability studies | **4** |
| 1.3 | Synthesis of europlatin (**1**) and terbiplatin (**2**) | **7** |
| **2** | **DNA binding methods** | |
| 2.1 | Absorption spectral studies | **7** |
| 2.2 | Ethidium bromide displacement assay | **8** |
| 2.3 | Circular dichroism studies | **8** |
| 2.4 | Isothermal titration calorimetry | **9** |
| 2.5 | Gel electrophoretic mobility shift assay | **10** |
| **3** | **BSA binding assay** | **11** |
| **4** | **Cell proliferation assay** | **11** |
| **5** | **Cellular uptake studies by confocal fluorescence microscopy** | **12** |
| **6** | **References** | **14** |
| **Scheme S1** | General synthetic scheme for complexes **1** and **2** | **15** |
| **Figure S1** | Time-dependent UV-visible spectral changes of complex **1** in water | **16** |
| **Figure S2** | ESI-MS spectral analyses of complex **1** | **16** |
| **Figure S3** | ESI-MS spectral analyses of complex **2** | **17** |
| **Table S1** | Assignments of the major peaks observed in the ESI-MS spectra of complexes **1** and **2** | **18** |
| **Figure S4** | UV-Visible spectra for complexes **1** and **2** in water | **19** |
| **Figure S5** | Photostability studies of SYTO®RNASelect™ and europlatin using emission spectroscopy | **20** |
| **Figure S6** | Photostability studies of SYTO®RNASelect™ and europlatin using electronic spectroscopy | **21** |
| **Figure S7** | Luminescence decay profile in presence of water and $D_2O$ for complexes **1** and **2** respectively | **22** |
| **Figure S8** | Absorption spectral traces of complex **1** in Tris-buffer with increasing the concentration of CT-DNA. Inset shows the plot of $\Delta\varepsilon_{af}/\Delta\varepsilon_{bf}$ vs. [DNA] | **23** |

| | | |
|---|---|---|
| **Figure S9** | Absorption spectral traces of complex **2** in Tris-buffer with increasing the concentration of CT-DNA. Inset shows the plot of $\Delta\varepsilon_{af}/\Delta\varepsilon_{bf}$ vs. [DNA] | **24** |
| **Figure S10** | Emission spectral traces of ethidium bromide bound CT-DNA with varying concentration of complex **1** in 5 mM Tris buffer with inset showing ($I/I_0$) vs. [complex] plot | **25** |
| **Figure S11** | Emission spectral traces of ethidium bromide bound CT-DNA with varying concentration of complex **2** in 5 mM Tris buffer with inset showing ($I/I_0$) vs. [complex] plot | **25** |
| **Figure S12** | ITC plot showing binding parameters for complex **2** with CT-DNA | **26** |
| **Figure S13** | Emission spectral traces of bovine serum albumin (BSA) protein in the presence of increasing concentration of complex **1** with inset showing ($I/I_0$) vs. [complex] plot | **27** |
| **Figure S14** | Emission spectral traces of bovine serum albumin (BSA) protein in the presence of increasing concentration of complex **2** with inset showing ($I/I_0$) vs. [complex] plot | **28** |
| **Table S2** | BSA binding parameters of complexes **1** and **2** | **29** |
| **Figure S15** | MTT assay of complexes **1** and **2** with HeLa and H460 cell line | **30** |
| **Figure S16** | Cellular internalization of complexes **1** and **2** in HeLa and H460 | **31** |
| **Figure S17** | Confocal fluorescence microscopic images of the HeLa, H460 and MCF7 cells showing the intracellular localization profile | **32** |
| **Figure S18** | Time-dependent confocal fluorescence microscopic images of the HeLa cells using **1**, **2** and SYTO® RNASelect showing their comparative photostability | **33** |

# 1. Experimental

## 1.1. Materials.

All the reagents including $Eu(NO_3)_3{\cdot}6H_2O$, $Tb(NO_3)_3.6H_2O$, 3-aminoquinoline, diethylene triaminepentaacetic acid (DTPA) and $K_2PtCl_4$ were purchased from commercial sources (Alfa Aesar, India; Sigma-Aldrich, U.S.A) and used without further purifications. Water used for all experiments were of Milli-Q grade. 3-(4,5-Dimethylthiazol-2-yl)-2,5-diphenyltetrazoliumbromide (MTT), trypsin–EDTA, Dulbecco's modified eagle's medium (DMEM, Gibco® Life Technologies, Bengaluru, India), penicillin–streptomycin antibiotic, bisBenzimide H33258, and gelatin (from cold water fish skin) were purchased from Sigma-Aldrich (Bengaluru, India) and used for as received. SYTO® RNASelect green fluorescent stain kit (Cat. No. S32703) was obtained from ThermoFisher Scientific. Supercoiled (SC) pUC19 DNA (CsCl purified) was purchased from Merck Millipore (India). Tris(hydroxymethyl)aminomethane−HCl (Tris-HCl) buffer solution (pH 7.2) was prepared from Milli-Q water of resistivity of 18.2 $M\Omega.cm^{-1}$. Calf thymus DNA (CT-DNA), bovine serum albumin (BSA), ethidium bromide (EthBr), agarose (molecular biology grade) methyl green, catalase, gel loading solution (containing 0.25% (w/v) bromophenol blue, 0.25% xylene cyanole FF and 40% sucrose in water) were purchased from Sigma (U.S.A.). *Cis*platin was prepared from $K_2PtCl_4$ according to known literature procedure.[S1] *cis*-$[Pt(NH_3)_2Cl(DMF)](NO_3)$ was synthesized from *cis*platin using a reported procedure.[S2] Ligand L (L = *N*,*N*′′-bis(3-amidoquinolyl) diethylenetriamine-*N*,*N*′,*N*′′-triacetic acid ) and precursor

lanthanide complexes, *viz*. [Ln(L)($H_2O$)] (Ln = Eu, Tb) were prepared using our earlier reported procedure.[S3]

## 1.2. Physical Methods.

The elemental microanalyses for C, H and N were performed using a Perkin-Elmer 2400 Series II elemental analyzer. FTIR spectra was achieved with a Perkin-Elmer Model 1320 FT-IR spectrometer (KBr disk, 400-4000 $cm^{-1}$). $^1$H-NMR spectra were collected at 298 K on a JEOL-ECX 500 FT (500 MHz) instrument with chemical shift referenced to tetramethylsilane (TMS = $Me_4Si$) as the internal standard. Electrospray ionization mass spectral (ESI-MS) measurements were performed using a WATERS Q-TOF Premier mass spectrometer. Electronic absorption spectra was recorded at 298 K using a Perkin-Elmer Lambda 25 UV-vis spectrophotometer. The circular dichroism (CD) spectroscopy of the complexes with CT-DNA were done by using JASCO J-815 spectropolarimeter equipped with a Peltier temperature control device under continuous flow of nitrogen purging. The fluorescence and time-delayed luminescence spectral data were achieved using Agilent Cary eclipse fluorescence spectrophotometer at 298 K. Lifetime measurements for europlatin (**1**) and terbiplatin (**2**) were done in Tris-buffer (pH 7.2, at 298 K) using a pulsed Xenon lamp at $\lambda_{ex}$ =315 nm for both with $\lambda_{em}$ =616 nm and 545 nm respectively with a delay time and gate time of 0.1 ms. Decay curves were fitted by non-linear least square method.

The excited state lifetime measurements in water and $D_2O$ allowed the determination of the number of water molecules ($q$) directly coordinated to the respective $Ln^{III}$ using the following modified Horrocks' equations for $Eu^{III}$ and $Tb^{III}$ respectively.[S4]

$$q_{\mathrm{Eu}} = 1.2\left(\frac{1}{\tau_{\mathrm{H_2O}}} - \frac{1}{\tau_{\mathrm{D_2O}}} - 0.25\right)$$

$$q_{\mathrm{Tb}} = 5.0\left(\frac{1}{\tau_{\mathrm{H_2O}}} - \frac{1}{\tau_{\mathrm{D_2O}}} - 0.06\right)$$

The overall luminescence quantum yields of the complexes were measured in Tris-HCl buffer (pH=7.2) at 298 K at room temperature according to a reported procedure using quinine sulfate as reference using following equation: [S5]

$$\emptyset_{\mathrm{overall}} = \emptyset_{\mathrm{ref}} A_{\mathrm{ref}} I n^2 / A I_{\mathrm{ref}} n^2_{\mathrm{ref}}$$

where *A*, *I* and *n* denote the respective absorbance at the excitation wavelength, area under the emission spectral curve and refractive index of the solvent respectively. The $\phi_{\mathrm{ref}}$ represents the quantum yield of the standard quinine sulfate solution for lanthanoplatins and fluorescein for SYTO® RNASelect™.

**Photostability experiments.**

Photostability is one of the most important criteria for suitability of fluorescent cellular imaging agents. We observed significant photobleaching or decrease in fluorescence intensity for free SYTO®RNASelect™ upon photoirradiation compared to europlatin (**1**). Similar photobleaching of free SYTO®RNASelect™ is well-known in literature.[S6] The photostability experiments was carried out in quartz cells (1 cm path length) using 30 µM solutions of SYTO®RNASelect™ and europlatin in buffer medium (5 mM Tris HCl-NaCl buffer, pH 7.2) at 298 K upon continuous irradiation of green LED light ( 490 nm-550 nm, 18 W) for 14 min. Both emission/luminescence spectra and electronic spectra was recorded at regular time interval upon irradiation for both SYTO®RNASelect™ and europlatin. The fluorescence intensity of SYTO®RNASelect™ was found to decreased by ~80% while the luminescence intensity of europlatin showed only ~10% reduction in intensity (Fig. S5). We have also observed significant changes in electronic spectra of SYTO®RNASelect™, which showed appreciable decrease in absorbance with shift in absorbance peak from 470 nm to 496 nm (Fig. S6. In

contrast there was almost no changes in absorbance spectra of europlatin upon photo-exposure. These observations strongly indicate remarkable photostability of lanthanoplatins compared to SYTO® RNASelect™, highly desirable parameter for fluorescent cellular imaging agents.

## 1.3. Synthesis of Compounds

### 1.3.4 Synthesis of [{*cis*-Pt($NH_3$)$_2$(Cl)}$_2$Ln(L)($H_2O$)]($NO_3$)$_2$ (Ln = Eu (1), Tb (2)):

To a 5 mL water-DMF mixture (9:1) having 0.307 mmol of [Ln(L)($H_2O$)] (Ln= Eu (0.250 g, 0.307 mmol), Tb ( 0.251 g, 0.307 mmol)) was added *cis*-[Pt($NH_3$)$_2$Cl(DMF)]($NO_3$) (0.254 g, 0.616 mmol). The reaction mixture was stirred at 50 $^oC$ in dark condition for 24 h to form a pale yellow colour clear solution. Excess of acetone (150 mL) was added to the reaction mixture which lead to a yellow colored precipitate. The resulting precipitate was filtered off, washed with cold diethyl ether and dried in vacuum over $P_4O_{10}$ to obtain the desired lanthanoplatins **1** and **2**, [{*cis*-Pt ($NH_3$)$_2$(Cl)}$_2$Ln(L)($H_2O$)]($NO_3$)$_2$ (Ln = Eu (**1**), Tb (**2**)).

**[{*cis*-Pt($NH_3$)$_2$Cl}$_2$Eu(L)($H_2O$)]($NO_3$)$_2$ (Europlatin, 1):** Yield: 0.364 g (74%). Anal. Calcd for $C_{32}H_{46}Cl_2EuN_{13}O_{15}Pt_2$: C, 26.22; H, 3.16; N, 12.42; Found: C, 26.38; H, 3.28; N, 12.62; FTIR (KBr pellet, $\nu_{max}$, $cm^{-1}$): 3423 (br, -OH), 3264 (m), 1605 (vs, $\nu_{asym}$ $CO_2^-$), 1595 (vs, C=O for –CONH), 1385 (s, $\nu_{sym}$ $CO_2^-$), 1331 (m), 1112 (s), 967 (m), 659 (m), 595 (s). UV-visible ($H_2O$, 298 K): $\lambda_{max}$, nm ($\varepsilon$, $M^{-1}cm^{-1}$): 243 (22,530), 315 (3,800). ESI-MS in $H_2O$: *m/z* 511.58 $[C_{32}H_{38}EuN_9O_8Pt]^{2+}$; 661.06 $[C_{32}H_{44}Cl_2EuN_{11}O_8Pt_2]^{2+}$; (See Table S1 for detailed mass spectral analysis). Molar conductivity in 10% aqueous DMF at 298 K [$\Lambda_M$/S $cm^2$ $mol^{-1}$]: 21.6.

**[{*cis*-Pt($NH_3$)$_2$(Cl)}$_2$Tb(L)($H_2O$)]($NO_3$)$_2$ (Terbiplatin, 2):** Yield: (0.350 g, 71%). Anal. Calcd for $C_{32}H_{46}Cl_2TbN_{13}O_{15}Pt_2$ is C, 26.10; H, 3.15; N, 12.36; Found: C, 26.32; H, 3.30; N, 12.54; FTIR (KBr pellet, $\nu_{max}$, $cm^{-1}$) 3430 (br, -OH), 3265, 1606 (vs, $\nu_{asym}$ $CO_2^-$), 1591 (vs, C=O for –CONH), 1387 (s, $\nu_{sym}$ $CO_2^-$), 1328 (m), 1135 (s), 965(m), 657 (m), 618(s). UV-visible ($H_2O$,

298 K): $\lambda_{max}$, nm ($\varepsilon$, $M^{-1}cm^{-1}$): 243 (19,600), 315 (3,800). ESI-MS in $H_2O$: *m/z* 665.05 $[C_{32}H_{44}Cl_2TbN_{11}O_8Pt_2]^{2+}$, 1066.14 $[C_{32}H_{39}TbN_9O_8Pt]^+$ (See Table S1 for detailed mass spectral analysis). Molar conductivity in 10% aqueous DMF at 298 K [$\Lambda_M$/S $cm^2$ $mol^{-1}$]: 28.6.

**2. DNA Binding Methods:** Binding assay of [{*cis*-$Pt(NH_3)_2(Cl)$}$_2$Ln(L)($H_2O$)] (Ln= Eu (**1**) Tb (**2**)) with CT-DNA were performed by UV-visible absorption titration, ethidium bromide (EthBr) displacement assay using emission spectroscopy, circular dichroism (CD), isothermal titration calorimetry (ITC) and agarose gel retardation assay.

**2.1. Absorption Spectral Studies.**

DNA binding assay was performed in Tris–HCl/NaCl buffer (5 mM Tris–HCl/NaCl, pH 7.2) using aqueous solution of the complexes **1** and **2**. In the buffer medium CT-DNA gave the ratio of 1.9:1 of absorbance in UV region at wavelength 260 and 280 nm which proved that DNA is free from protein. DNA concentration was calculated through known molar extinction coefficient at 260 nm ($\varepsilon_{260}$ = 6600 $M^{-1}$ $cm^{-1}$).[S7] Absorption spectral titrations were carried out by increasing the concentration of CT-DNA while keeping the complex concentration constant. Corrections made for the absorbance value of CT-DNA itself. The equilibrium binding constant ($K_b$) of the complexes was achieved by the following equation.[S8]

$$[DNA]/(\varepsilon_a - \varepsilon_f) = [DNA]/(\varepsilon_b - \varepsilon_f) + 1/K_b(\varepsilon_b - \varepsilon_f)$$

where [DNA] is the concentration of CT DNA in the base pairs, $\varepsilon_a$ is the apparent extinction coefficient, $\varepsilon_f$ and $\varepsilon_b$ refers to the extinction coefficients of the complex in its free and fully bound form. The $K_b$ values are obtained from the [DNA]/($\varepsilon_a - \varepsilon_f$) *vs.* [DNA] plots.

**2.2. Ethidium Bromide Displacement Assay.**

The apparent binding constant ($K_{app}$) of the complexes **1** and **2** with CT DNA was calculated from the emission spectral measurements using ethidium bromide (EthBr) as a spectral probe

in 5 mM Tris-HCl/NaCl buffer (pH 7.2) at 298 K. The fluorescence quenching of free EthBr by solvent molecules in Tris-buffer medium results in no apparent emission. The intercalative binding of CT-DNA significantly enhances the emission intensity of EthBr.

The competitive binding ability of the complexes **1** and **2** to DNA was estimated from the reduction of the emission intensity. The apparent binding constant (*K*app) were obtained by the following equation:[S9]

$K_{app}$ x $[Complex]_{50}$ = $K_{EthBr}$ x [EthBr]

Where $K_{app}$ is the apparent binding constant of the complex. $[Complex]_{50}$ is the concentration of the complex at 50% quenching of DNA-bound ethidium bromide emission intensity, $K_{EthB}$ is the binding constant of the EthBr ($K_{EthBr}$ = 1.0 x $10^7$ $M^{-1}$), and [EthBr] is the concentration of ethidium bromide (4.0 $\mu$M).

**2.3. Circular Dichroism Studies.**

The circular dichroism (CD) spectroscopy of CT-DNA in presence/absence of the complexes were performed by using JASCO J-815 spectropolarimeter equipped with a Peltier temperature control device at 298 K under continuous flow of nitrogen purging. All the experiments were carried out in a 1-mm path length quartz cell. CD spectra of CT-DNA in absence and presence of the complexes at various molar ratio of [complex]/[CT-DNA] were recorded after incubation with CT-DNA at 37 $^{o}$C for 6 h. Each spectra was recorded in 5 mM Tris-HCl/NaCl buffer (pH 7.2) by the accumulations of three average spectra and subtracting the data of the buffer with a scan speed 100 nm $min^{-1}$.

**2.4. Isothermal Titration Calorimetry (ITC) Study.**

ITC experiment was carried out to study the binding interaction of the complexes **1** and **2** with CT- DNA in Tris- HCl/NaCl buffer (5 mM Tris-HCl, 5 mM NaCl, pH 8.5). The experiment

was performed by using MicroCal iTC200 system at 30 $^{0}$C. All solutions were completely degassed before starting the experiment. The reference cell solution and the sample cell solution should possesses the same heat capacity. The sample cell thoroughly washed with Tris-HCl/NaCl buffer before starting the experiment. 0.01 mM CT-DNA was loaded in the sample cell. The heat released by dilution of CT- DNA by buffer in the cell is negligible. Complexes (0.1 mM) were dissolved in Tris-HCl/NaCl buffer (5 mM Tris-HCl, 5 mM NaCl, pH 8.5) and injected in the sample cell. Titration was performed by using a 40 $\mu$L syringe filled with the complex solution, with stirring at 1000 rpm. Injections were initiated after baseline stability was achieved. A titration experiment consisted of 20 consecutive injections of 2 $\mu$L volume and 4 sec duration each, with a filter period of 5 sec. The reference power was set at 5 $\mu$cal/sec with an initial delay of 60 sec. The resulting data were fitted by two set of binding model using MicroCal® ORIGIN software supplied with the instrument.

**2.5. Gel Electrophoretic Mobility Shift Assay (EMSA).**

The determination of the unwinding of closed circular, supercoiled pUC19 plasmid DNA induced by the complexes differing in their coordination mode with the DNA double helix was done by gel electrophoretic mobility shift assay (EMSA). Supercoiled pUC19 DNA (0.2 $\mu$g) was treated with different concentrations of the respective complexes (10, 20, 40, 60, 80 μM) in 50 mM Tris-HCl/NaCl buffer (pH 7.2) to a dilution to 20 $\mu$L final volume using Tris-HCl buffer. The mixtures were incubated in dark at 37 $^{o}$C for 12 h, and finally, 2 $\mu$L of loading buffer containing 0.25% bromophenol blue, 0.25% xylene cyanol FF and 40% sucrose was added for quenching. The solutions were finally loaded on 1% agarose gel and electrophoresed in a dark room for 2.0 h at 60 V in TAE gel running buffer. After electrophoresis gel was stained with 1.0 $\mu$g/mL ethidium bromide the bands were visualized by UV-A light and image was taken by using UVITEC FireReader V4 gel documentation system.

**3. BSA Interaction assay:** The study of the protein interaction was carried out by tryptophan fluorescence quenching experiment by using BSA (2 $\mu$M) in Tris-HCl buffer (pH 7.2). The tryptophan emission quenching was monitored ($\lambda_{ex}$ = 295 nm) by using complexes **1** and **2** with increasing concentrations. The quenching constant ($K_{BSA}$) has been determined quantitatively by using Stern-Volmer equation. Linear fitting was done by using the equation: $I_o/I = 1 + K_{BSA}[Q] = 1 + k_q \tau_o[Q]$.

Where $I_o$ and $I$ are the steady state emission intensities in the absence and presence of the quencher with concentration [Q]. $k_q$ is the quenching rate constant. Tryptophan average life time ($\tau_o$) without quencher has been reported as 1 x $10^{-8}$ s.[S9] The binding constant ($K$) and the number of binding sites ($n$) for such static quenching interaction can be determined using the Scatchard equation: [S10]

$$\log (I_o - I)/ I = \log K + n \log[Q]$$

The slope and the intercept of the double logarithm regression curve of $\log(I_o - I)/ I$ *versus* $\log[Q]$ gives the value for $n$ and $K$. (Figures S13 and S14). The various binding parameters for interaction of complexes **1** and **2** with BSA are listed in following Table S2.

**4. Cell Proliferation Assay.**

Complexes **1** and **2** were studied for their cell viability by colorimetric MTT (3-(4,5-dimethylthiazol-2-yl)-2,5-diphenyltetrazolium bromide) metabolic assay.[S11] The cytotoxicity assay was carried out in HeLa (human cervical carcinoma) and H460 (human lung carcinoma) cells. Maintenance of the cell was done with Dulbecco's minimum essential medium (DMEM) supplemented with 10% fetal bovine serum (FBS) in a humidified incubator at 37 °C with 5% $CO_2$. In 96 well tissue culture plates $10^4$ cells/well were plated onto multiple glass bottom at an initial confluence of ~70%. The cells were further treated with complexes **1** and **2** respectively. The cells were then treated with complexes dissolved in DMEM containing 1% DMSO at various concentrations for overnight (16 h) at 37 °C in a 5% $CO_2$ humidified

incubator. In dark room 0.5 mg/mL of MTT was prepared in Basal DMEM. 200 $\mu$L of the freshly prepared MTT solution was added to each of the cell containing wells, after discarding the old media, followed by incubation for 4-5 h in dark at 37 °C, in a 5% $CO_2$ humidified incubator. After the completion of incubation, the culture media was removed and DMSO (200 $\mu$L) was added to dissolve the formazon crystals by slowly shaking the plates for atleast 30 min. The cell proliferation was determined by measuring the absorbance at 570 nm by microtiter plate reader (Multiskan spectrum, Thermoscientific). This assay was repeated in triplicates. The values for percentage cell proliferation were normalized relative to untreated cells and a graph was drawn between percentage cell proliferation and concentration of the complexes to determine $IC_{50}$ values.

**5. Cellular Uptake Studies.**

Complexes **1** and **2** (25 μM) were added to the respective cell media, DMEM and sterilized by filtration with 0.22 micron filter. The HeLa cells (1 x $10^4$ cells/well) were seeded in 24 well plate (13 mm, 0.2% gelatin coated) containing sterilized glass cover slip till the confluency reached around 70%. Complexes were added in the cells and were incubated for 4 hours at 37 $^oC$ in a 5% $CO_2$-humidified incubator. And these cells were washed with 1X PBS buffer three times in an interval of 5 min to remove the debris then these cells were fixed with 4% formaldehyde solution for 20 min at room temperature. Subsequently, fixed slides were washed with 1X PBS buffer three times to remove the excess formaldehyde. The excess of formaldehyde in the fixed slide were removed by washing three times with 1X PBS buffer. After this, Hoechst 33258 was used to stain the nuclei of the cells for 15 min at room temperature and then washed with 1X PBS buffer in similar manner to remove the excess stain. The labeling and colocalization experiments with SYTO® RNASelect green fluorescent dye was performed adopting protocols mentioned in the kit using 0.5 μM labeling solution. Slides were coated with buffered mounting medium to prevent fading and drying followed by

mounted with the cover slips. The slides were observed and images were clicked using a Carl Zeiss LSM780NLO confocal laser scanning microscope (CLSM) at 40X magnification using appropriate filters for blue, red and green emission from Hoechst 33258, complexes **1** and **2.** The fluorescence imaging acquisition settings for europlatin (**1**): $\lambda_{ex}$ = 405 nm, emission filter: MBS 561, Laser: DPPS; for Hoechst 33258: Emission filter: MBS 760+, Laser: Chameleon; terbiplatin (**2**): $\lambda_{ex}$ = 488 nm, emission filter: MBS 488, Laser: Argon. To determine possible uptake mechanism, different inhibitors were used that inhibit specific endocytic pathways. Here we used filipin-III and genistein which inhibits caveolar mediated pathway, chloropromazine and nocodazole as inhibitors for clatherin-mediated pathway, rottlerin which inhibits macropinocytosis and cytochalasin-D which inhibits actin polymerization. HeLa cells ($10^4$ cells/well) were pre-treated with these inhibitors for 1 h, followed by incubation with terbiplatin (**2**) for 4 h. The CLSM images (Figure 5 in manuscript) indicate significant inhibition of uptake of complex **2** with rottlerin, indicating possible macropinocytosis-mediated pathway is involved in internalization of these complexes.[S12]

**References:**


S1. S. C. Dhara, *Indian J. Chem.*, 1970, **8**, 193-194.

S2. D. Fan, X. Yang, X. Wang, S. Zhang, J. Mao, J. Ding, L. Lin and Z. Guo, *J. Biol. Inorg. Chem.*, 2007, **12**, 655-665.

S3. K. Singh, S. Banerjee and A. K. Patra, *RSC Adv.*, 2015, **5**, 107503-107513.

S4. W. D. Horrocks and D. R. Sudnick, *J. Am. Chem. Soc.*, 1979, **101**, 334-340; A. Beeby, I. M. Clarkson, R. S. Dickins, S. Faulkner, D. Parker, L. Royle, A. S. de Sousa, J. A. G. Williams and M. Woods, *J. Chem. Soc., Perkin Trans.*, **2**, 1999, 493-504.

S5. A. T. H. Williams, S. A. Winfield and J. N. Miller, *Analyst*, 1983, **108**, 1067-1071.

S6. G. Song, Y. Sun, Y. Liu, X. Wang, M. Chen, F. Miao, W. Zhang, X. Yu and J. Jin, *Biomaterials*, 2014, **35**, 2103-2112; Y.-J. Lu, Q. Deng, D.-P. Hu, Z.-Y Wang, B.-H. Huang, Z.-Y. Du, Y.-X. Fang, W.-L. Wong, K. Zhang and C.-F. Chow, Chem. Commun., 2015, 51, 15241-15244.

S7. M. E. Reichmann, S. A. Rice, C. A. Thomas and P. Doty, *J. Am. Chem. Soc*., 1954, **76**, 3047-3053.

S8. A. Wolfe, G. H. Shimer and T. Meehan, *Biochemistry*, 1987, **26**, 6392-6396.

S9. M. Lee, A. L. Rhodes, M. D. Wyatt, S. Forrow and J. Hartley, *Biochemistry*, 1993, **32**, 4237-4245.

S10. J. R. Lakowicz, *Principles of Fluorescence Spectroscopy*, Springer, New York, 3rd edn, 2006.

S11. T. Mosmann, *J. Immunol. Methods*, 1983, **65**, 55-63.

S12. L. Yang, L. Shang and G. U. Nienhaus, *Nanoscale*, 2013, **5**, 1537−1543.

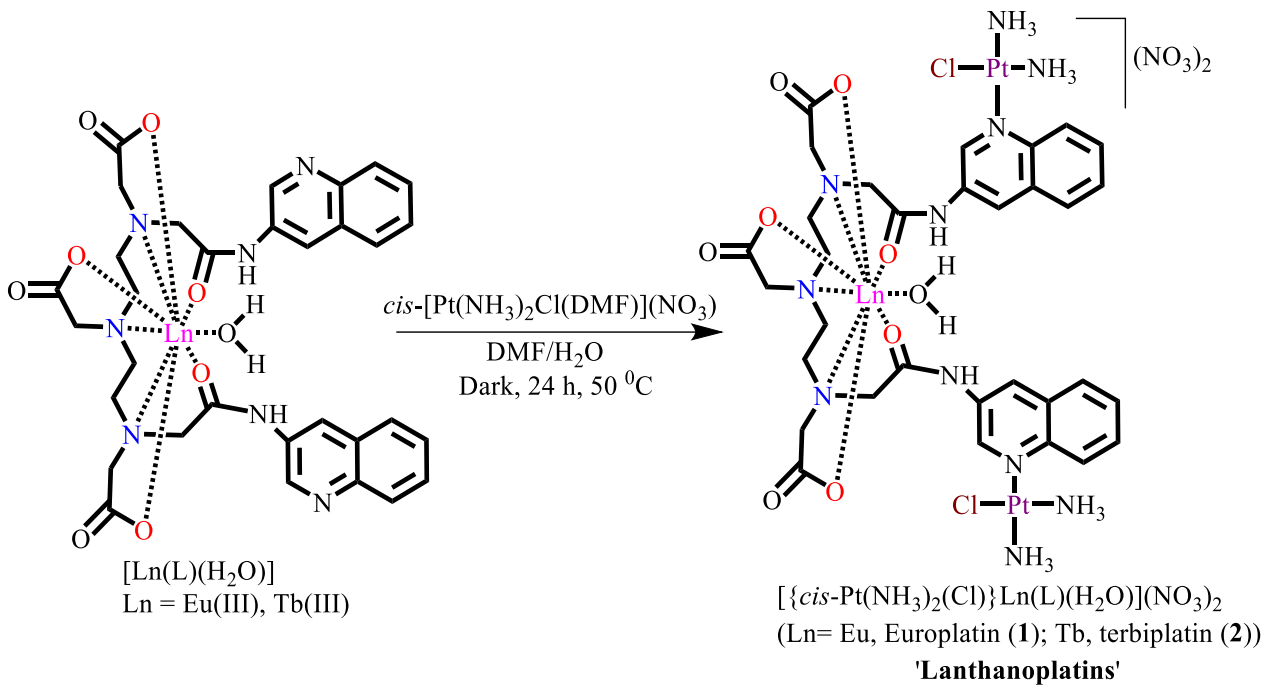


**Scheme S1:** General synthetic scheme for preparation of [{*cis*-Pt $(NH_3)_2(Cl)\}_2Ln(L)(H_2O)](NO_3)_2$ (Ln = Eu (**1**), europlatin; Tb (**2**), terbiplatin).

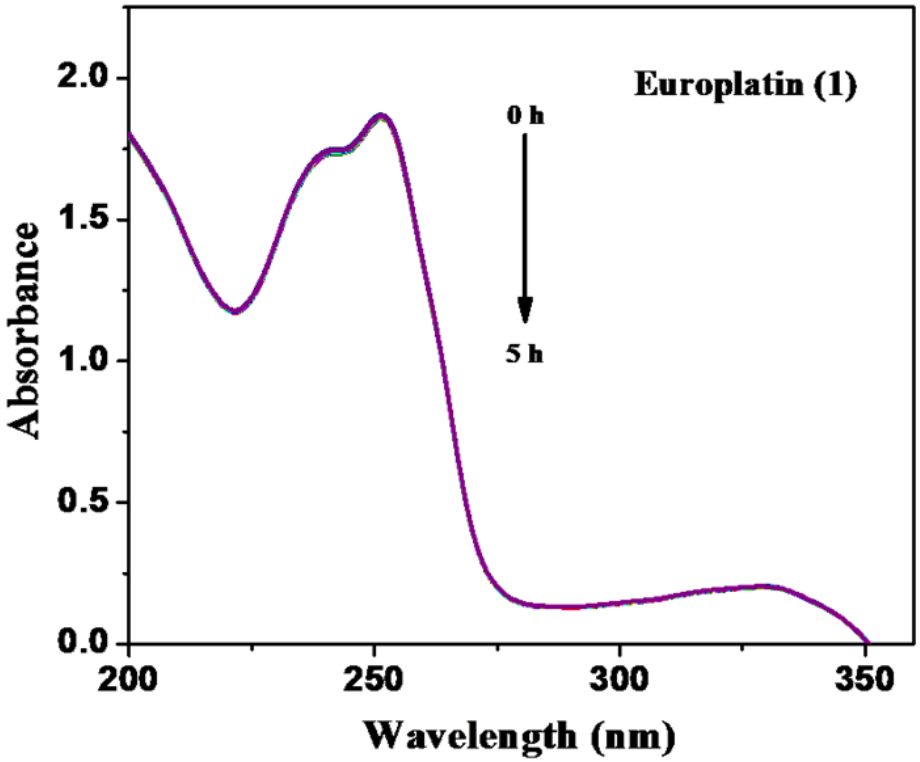


**Figure S1.** Time-dependent absorption spectral traces of europlatin (**1**) monitored for 5 h in water at 25 $^{o}$C to access the stability of the complexes in solution.

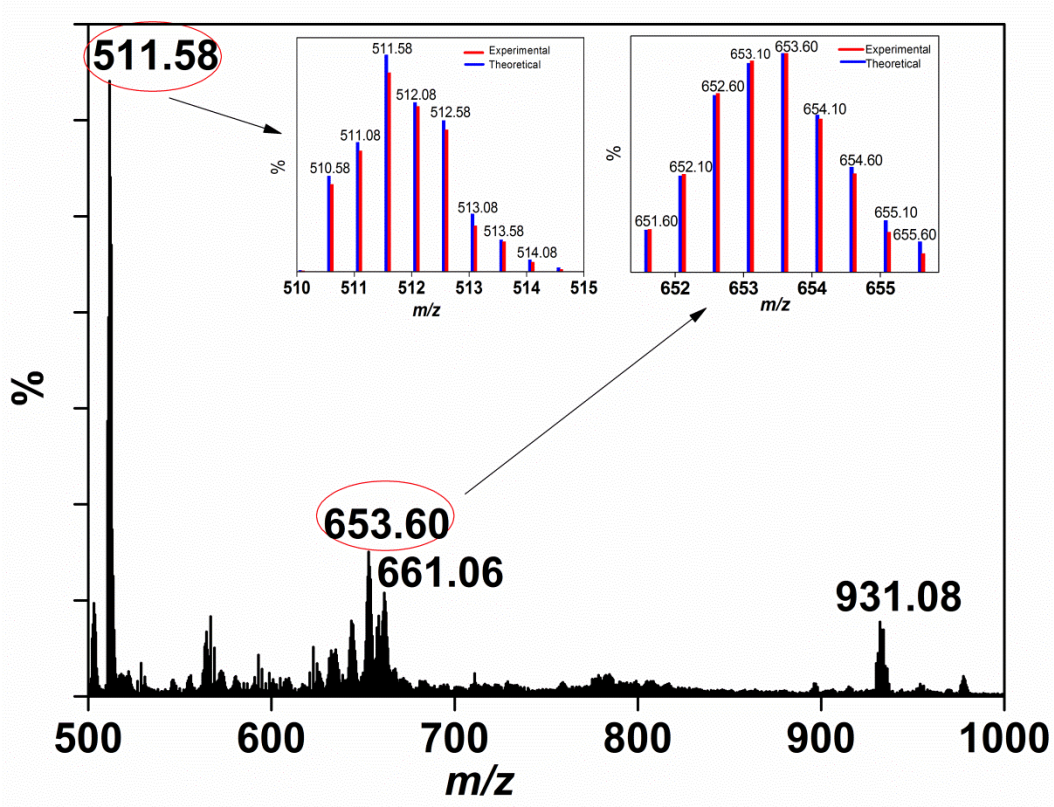


**Figure S2.** ESI-MS spectra of complex **1** in aqueous medium. Inset shows the experimental and theoretically simulated isotopic distribution patterns of the observed peaks at *m/z* 511.58 and *m/z* 653.60. See Table S1 for detailed analyses.

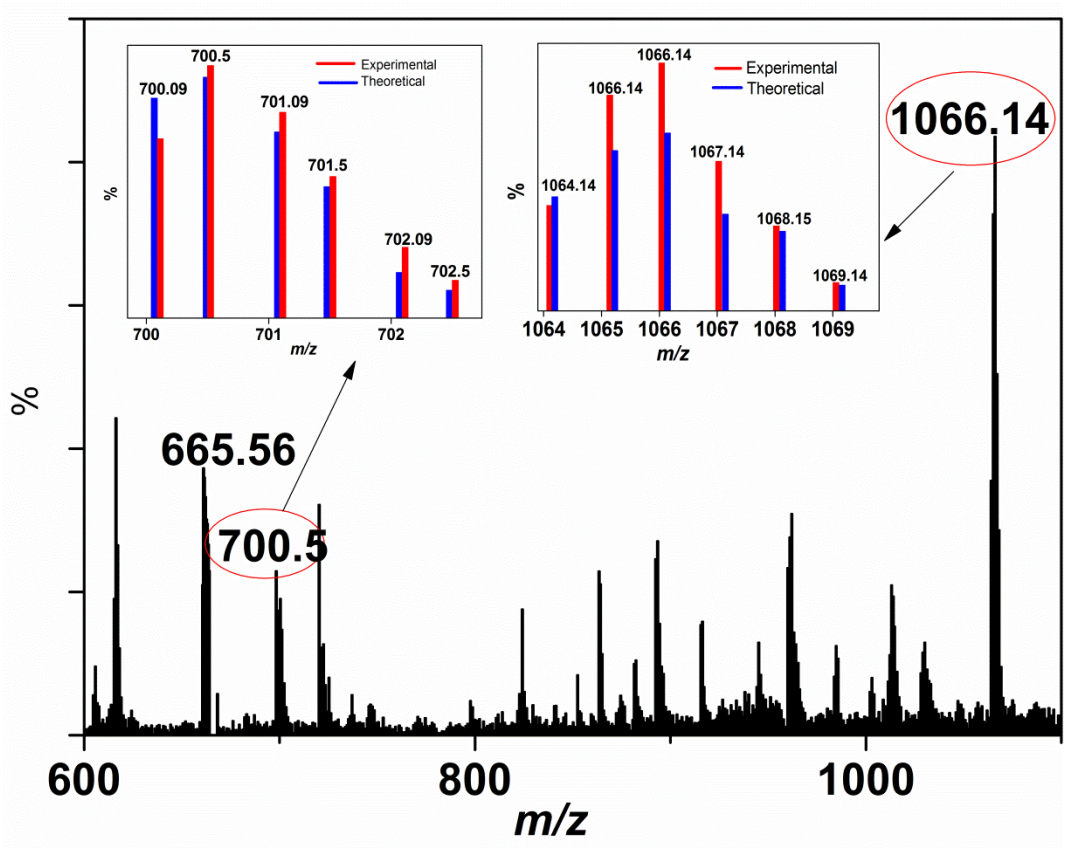


**Figure S3.** ESI-MS spectra of complex **2** in aqueous medium. Inset shows the experimental and theoretically simulated isotopic distribution patterns of the observed peaks at *m/z* 700.5 and *m/z* 1066.14. See Table S1 for detailed analyses.

**Table S1:** Assignments of the major peaks observed in the ESI-MS spectra of complexes **1** and **2** to corresponding assigned molecular fragments/species.

| Complex | Attribution | Molecular formula | Observed (*m/z*) | Calculated (*m/z*) |
|---|---|---|---|---|
| **1** | [**1**-2$NO_3$-$H_2O$]$^{2+}$ | [$C_{32}H_{44}Cl_2EuN_{11}O_8Pt_2$]$^{2+}$ | 661.06 | 661.06 |
| | [**1**-2Cl-2$NO_3$+3$H_2O$]$^{2+}$ | [$C_{32}H_{50}EuN_{11}O_{11}Pt_2$]$^{2+}$ | 653.60 | 653.61 |
| | [**1**-Pt($NH_3$)$_2$Cl-Cl-2$NO_3$-$H_2O$]$^{2+}$ | [$C_{32}H_{38}EuN_9O_8Pt$]$^{2+}$ | 511.58 | 511.58 |
| **2** | [**2**-2$NO_3$-$H_2O$]$^{+}$ | [$C_{32}H_{44}Cl_2TbN_{11}O_8Pt_2$]$^{2+}$ | 665.56 | 665.5 |
| | [**2**-2Cl +2$NO_3$+$H_2O$]$^{2+}$ | [$C_{32}H_{46}TbN_{13}O_{15}Pt_2$]$^{2+}$ | 700.40 | 700.6 |
| | [**2**-Pt($NH_3$)$_2$Cl-2$NO_3$-$H_2O$]$^{+}$ | [$C_{32}H_{39}ClTbN_9O_8Pt$]$^{+}$ | 1066.14 | 1066.14 |

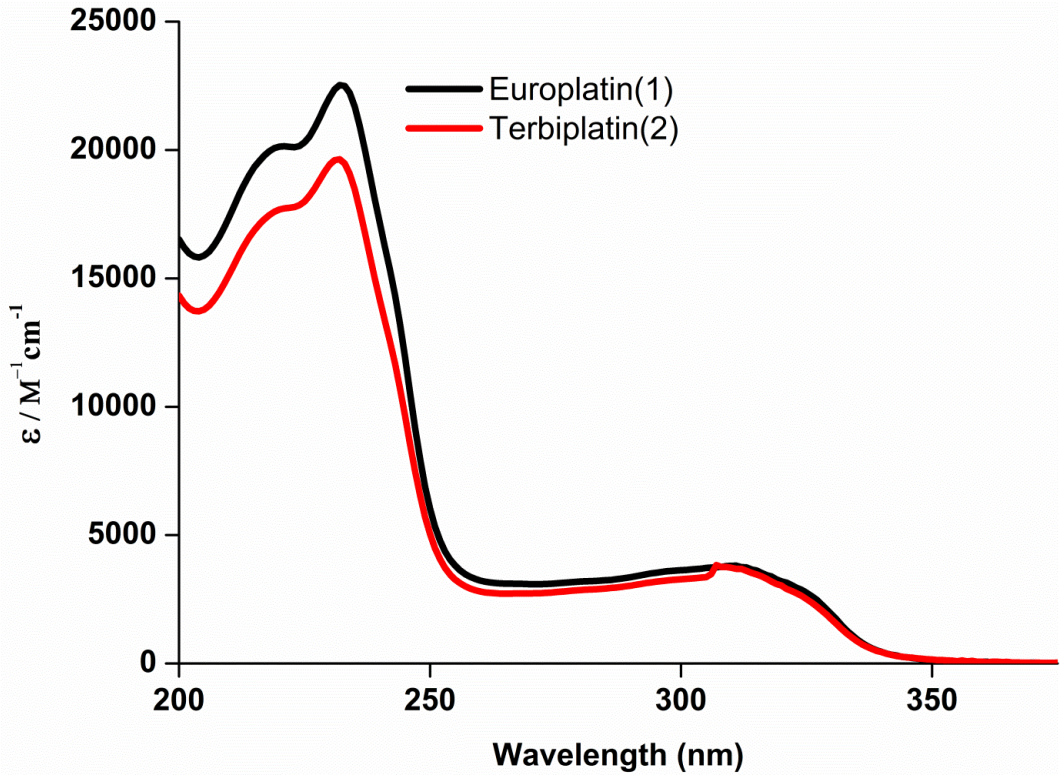


**Figure S4.** UV-visible absorption spectra of a 0.1 mM solution of complexes **1** and **2** in aqueous medium at pH 7.2 at 298 K.

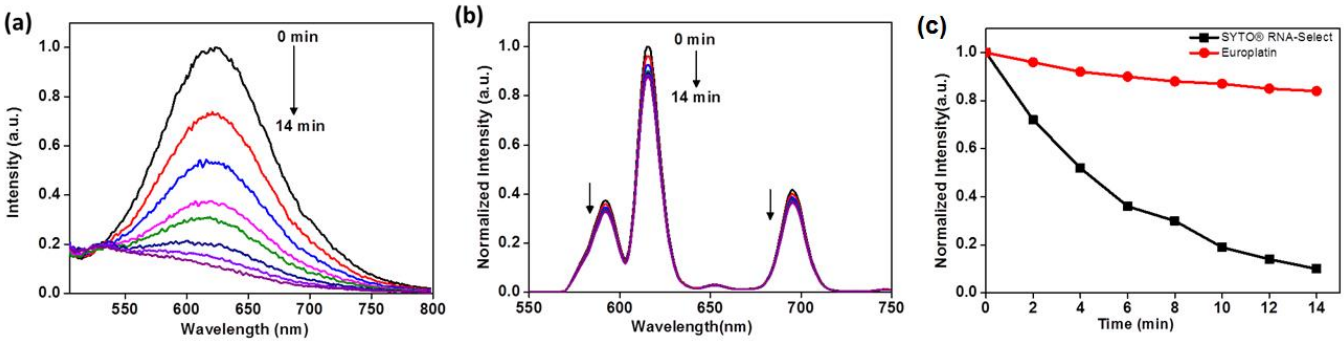


**Figure S5.** Photostability study with the quantitative analysis of the change in fluorescence spectra of (a) SYTO®RNASelect™ (30 µM; $\lambda_{ex}$ = 490 nm) and (b) europlatin (30 µM) in 5 mM Tris HCl-NaCl buffer (pH 7.2, 298 K) upon continuous irradiation of green LED light (490 nm- 550 nm, 18 W). (c) Comparative analysis of the changes in emission intensity of europlatin (**1**) and SYTO®RNASelect™.

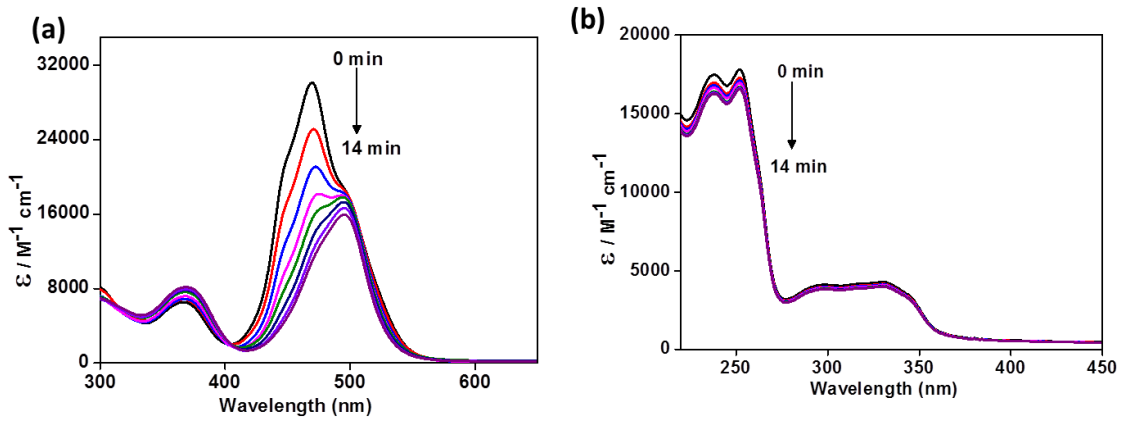


**Figure S6.** Photostability study with the analysis of the changes in the absorbance spectra of (a) SYTO®RNASelect™ and (b) europlatin (**1**) in 5 mM Tris HCl-NaCl buffer (pH 7.2, 298 K) upon continuous irradiation of green LED light (490 nm- 550 nm, 18 W).

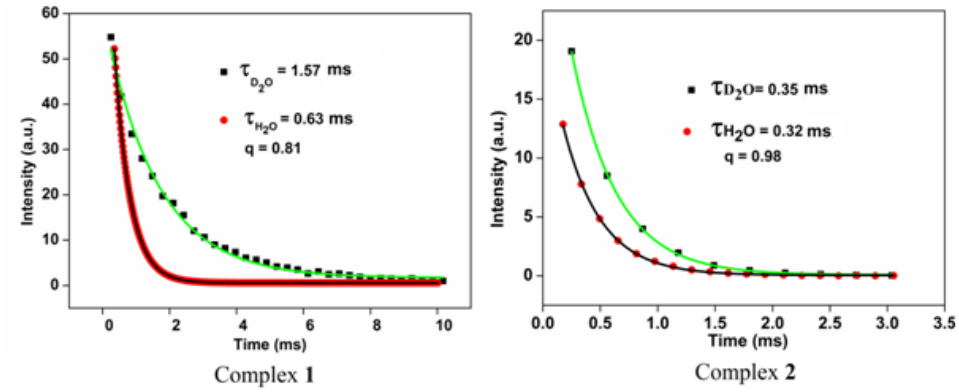


**Figure S7**. Luminescence decay profile from $^5D_0$ and $^5D_4$ states at 616 nm and 545 nm for $Eu^{3+}$ and $Tb^{3+}$ of complexes **1** and **2** (0.1 mM) respectively in water and $D_2O$ at 298 K (delay time = gate time = 0.1 ms). Data is fitted by single exponential fit with standard deviation of ± 10%. *q* is the number of water molecule coordinated to $Ln^{3+}$ ion in solution or hydration number measured from modified Horrock's equation.[S4]

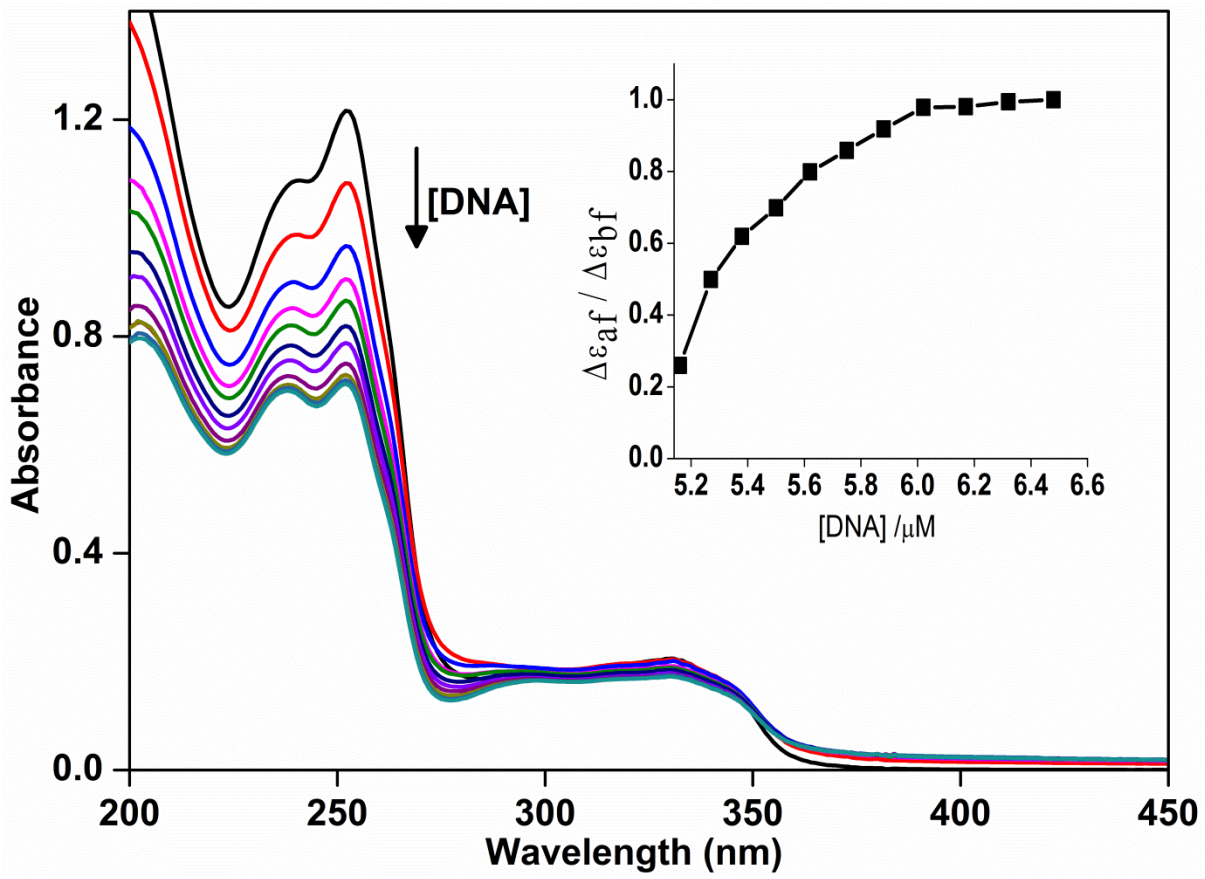


**Figure S8.** Absorption spectral traces of complex **1** in 5 mM Tris-HCl buffer at pH 7.2 with increasing the concentration of CT-DNA to the solution containing complex **1**. Inset shows the plot of $\Delta\varepsilon_{af}/\Delta\varepsilon_{bf}$ vs. [DNA].

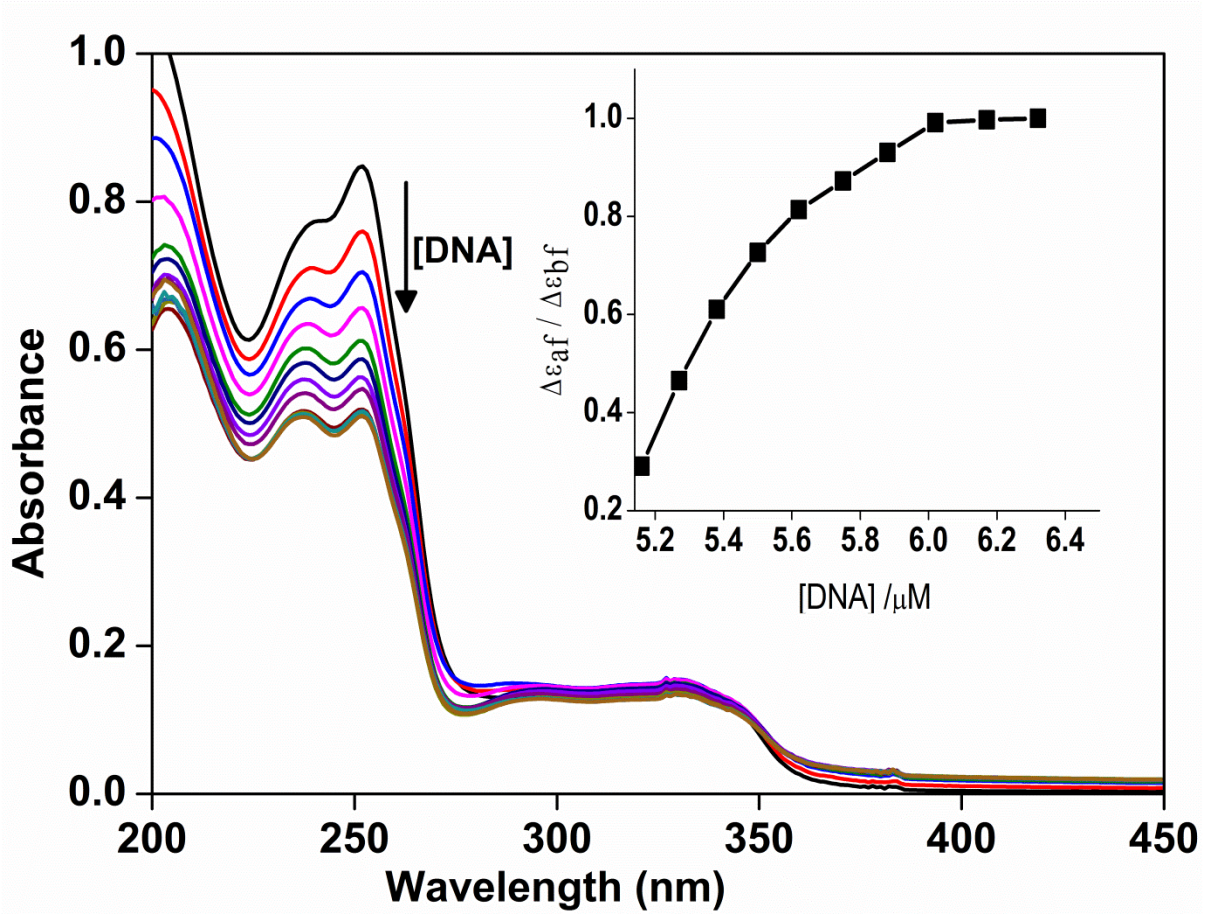


**Figure S9.** Absorption spectral traces of complex **2** in 5 mM Tris-HCl buffer at pH 7.2 with increasing the concentration of CT-DNA to the solution containing complex **2**. Inset shows the plot of $\Delta\varepsilon_{af}/\Delta\varepsilon_{bf}$ vs. [DNA].

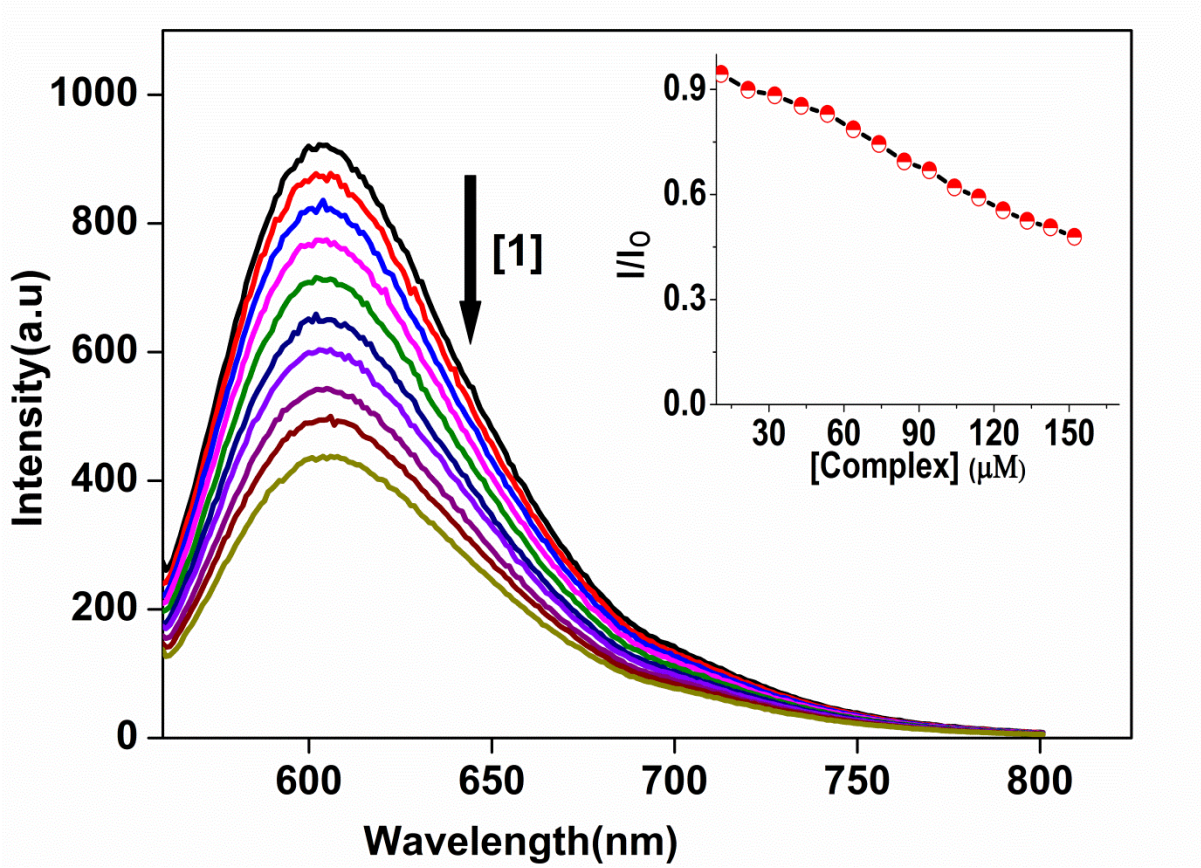


**Figure S10.** Emission spectral overlay plot for CT- bounded ethidium bromide (4 $\mu$M) in Tris-HCl buffer (5 mM, pH 7.2) with increasing concentration of complex **1**.

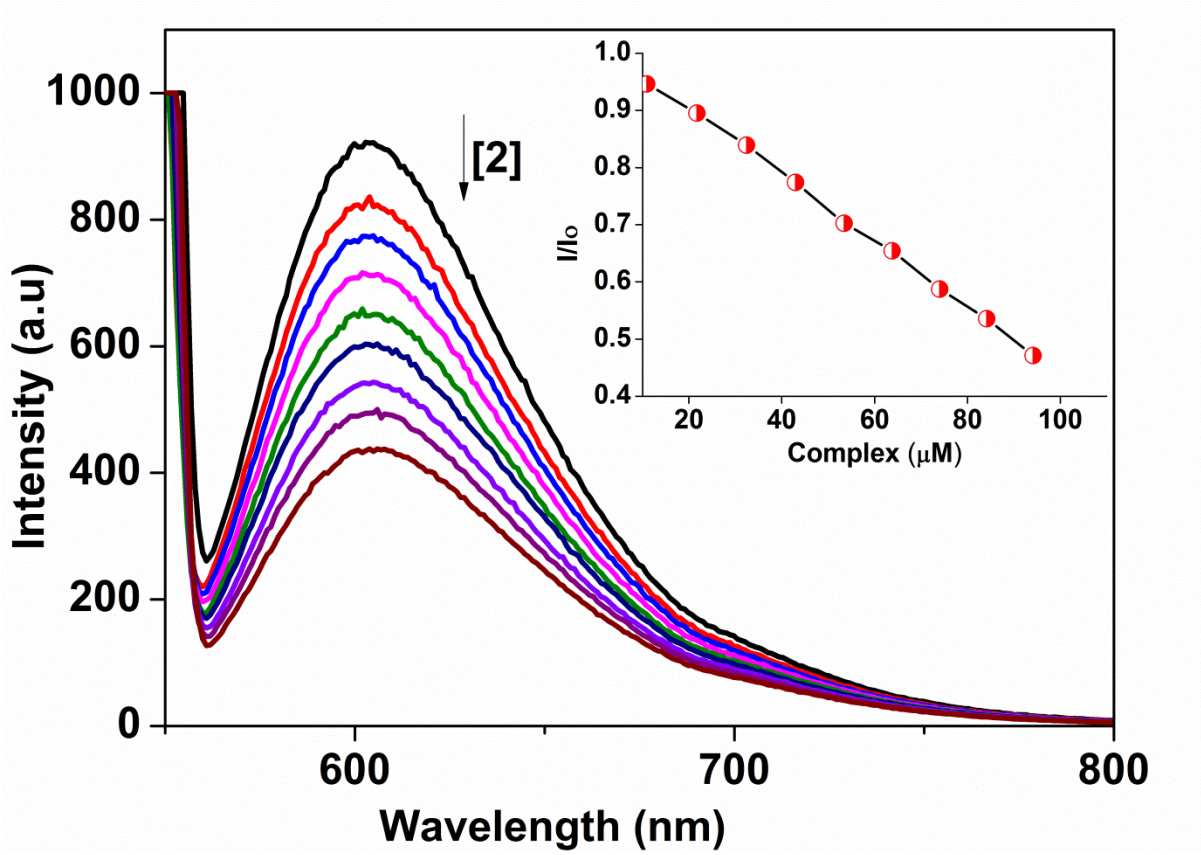


**Figure S11.** Emission spectral overlay plot for CT- bounded ethidium bromide (4 $\mu$M) in Tris -HCl buffer (5 mM, pH 7.2) with increasing concentration of complex **2**.

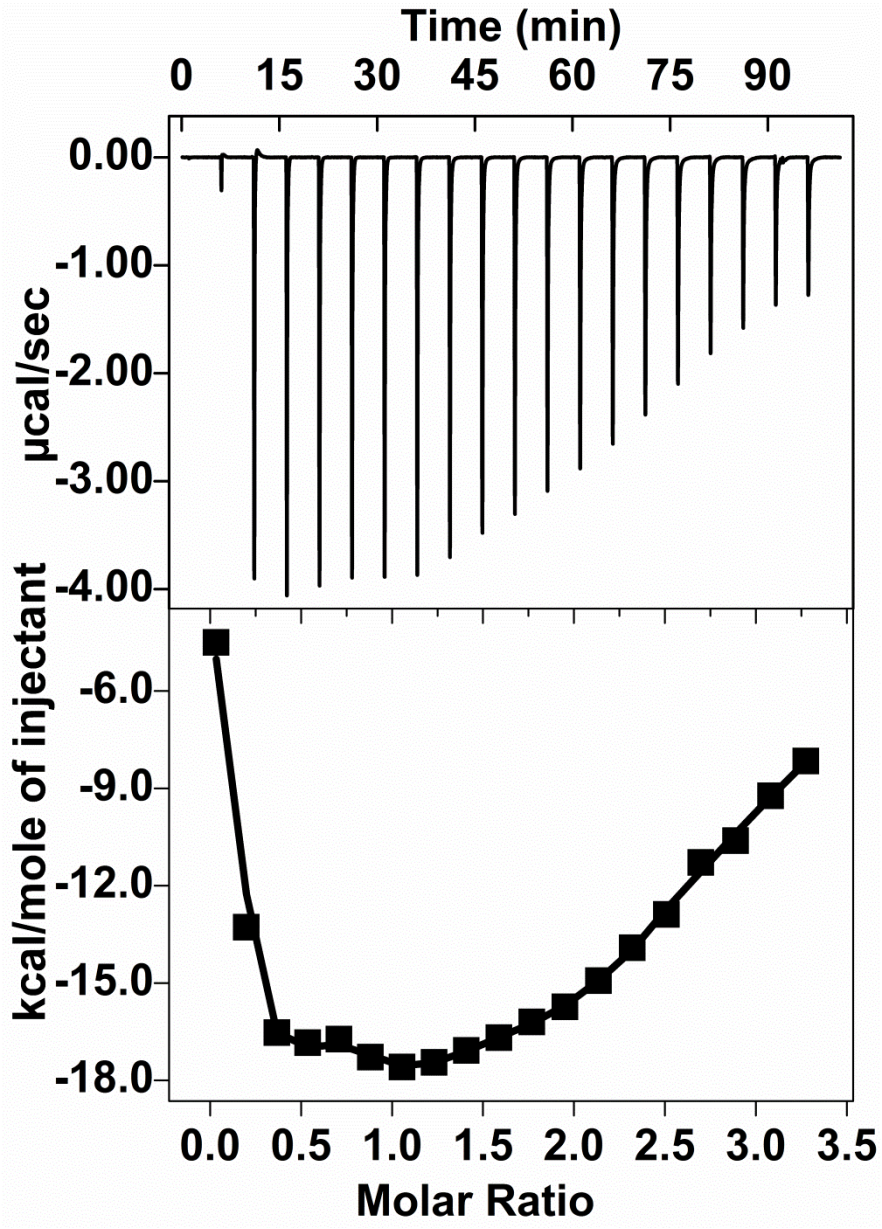


**Figure S12.** ITC profile for complex **2** (0.1 mM) when treated with CT-DNA (0.01 mM) at 30 $^{o}$C in 5 mM Tris HCl-NaCl buffer at pH 7.2. Fitting of the data points are done by two set of sites model. The calculated affinity constant (*K*) are $K_1$= 2.07 x $10^5$ $M^{-1}$, $K_2$ = 2.19 x $10^6$ $M^{-1}$.

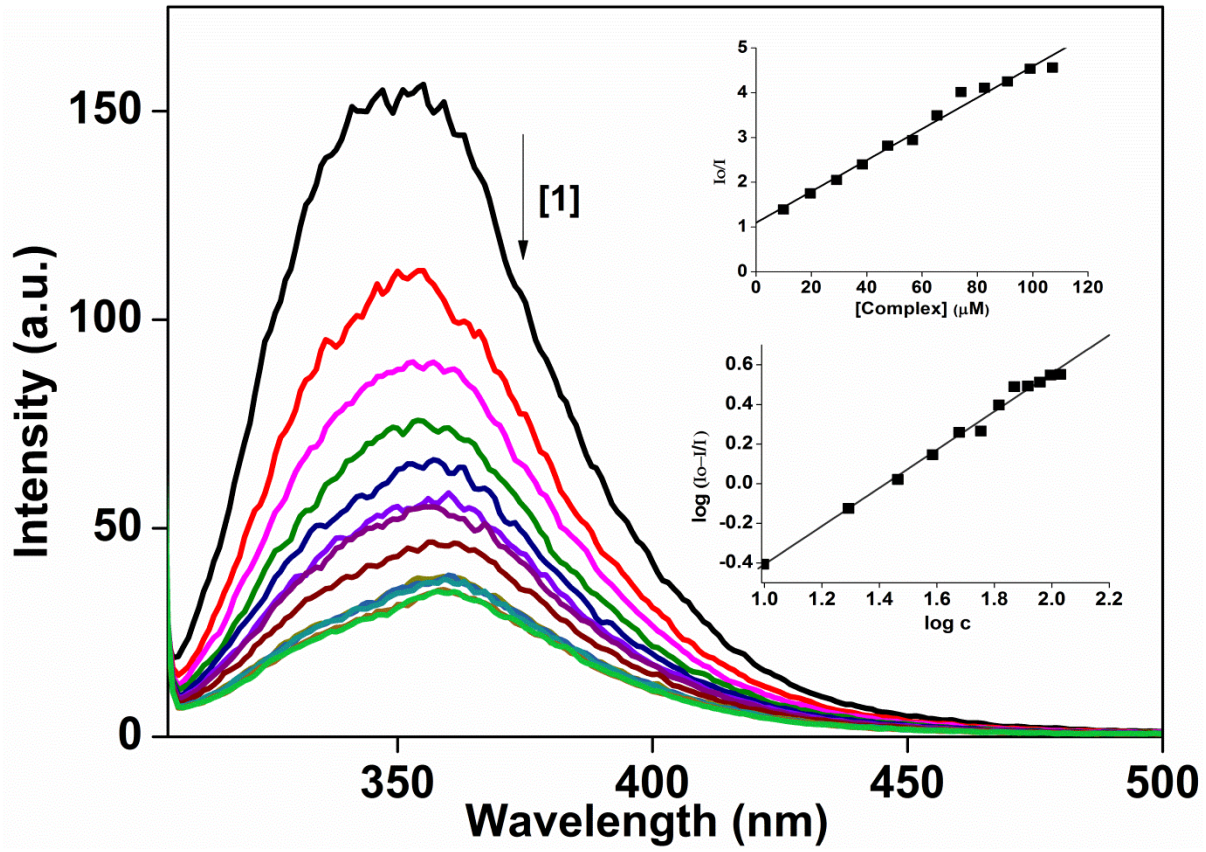


**Figure S13.** The effect of increasing concentration of complex **1** on the fluorescence quenching of BSA (2 $\mu$M) in Tris HCl- NaCl (5mM, pH 7.2). $\lambda_{ex}$ = 295 nm, $\lambda_{em}$ = 354 nm. The Inset figure shows (upper) the plot of $I_0/I$ *vs.* [complex] and (lower) the plot of log ($I_o$-$I/I$) *vs.* log $C$ where $C$ = quencher concentration.

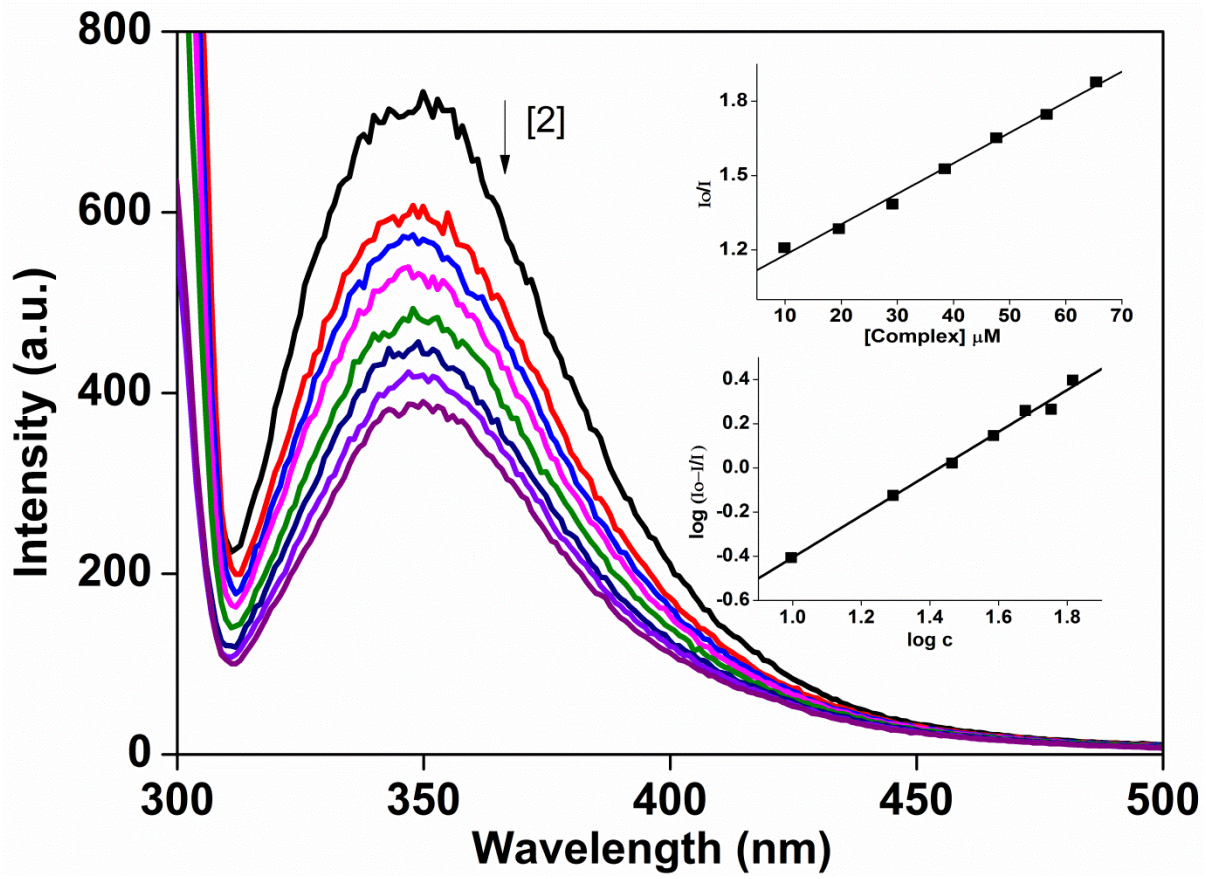


**Figure S14.** The effect of increasing concentration of complex (**2**) on the fluorescence quenching of BSA (2 $\mu$M) in Tris HCl- NaCl (5 mM, pH 7.2). $\lambda_{ex}$ = 295 nm, $\lambda_{em}$ = 350 nm. The Inset figure shows (upper) the plot of $I_0/I$ *vs.* [complex] and (lower) the plot of log ($I_o$-$I/I$) *vs* log $C$ where $C$ = quencher concentration.

**Table S2:** BSA binding parameters of complexes **1** and **2**:

| Complex | $K_{SV}$ ($M^{-1}$) | $K_q$ ($M^{-1}S^{-1}$) | $K$ ($M^{-1}$) | $n$ |
|---|---|---|---|---|
| **1** | 3.29 X$10^4$ | 3.29X$10^{12}$ | 2.6X$10^4$ | 0.96 |
| **2** | 1.69 X $10^4$ | 1.69X$10^{12}$ | 4.1X$10^4$ | 0.83 |

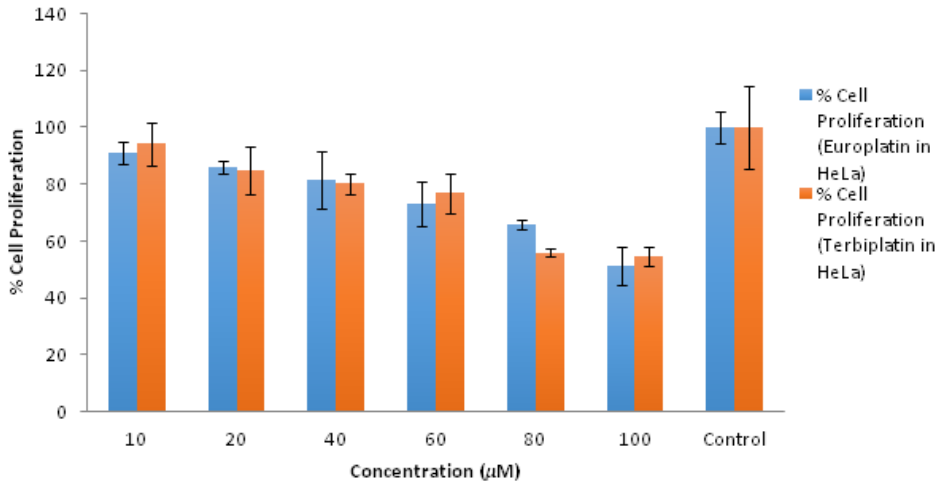


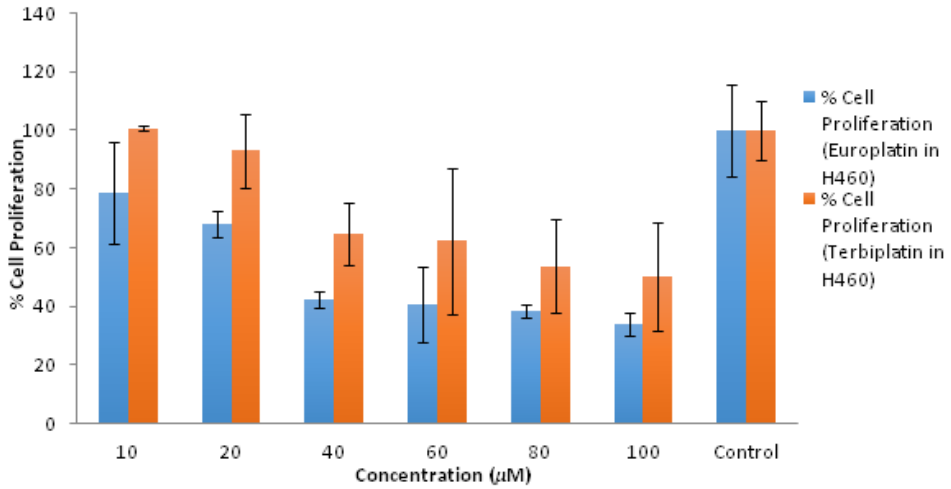


**Figure S15.** MTT cytotoxicity assay of complexes **1** (europlatin) and **2** (terbiplatin) at various concentration with HeLa (upper figure) and H460 cells (lower figure) upon incubation for 16 h.

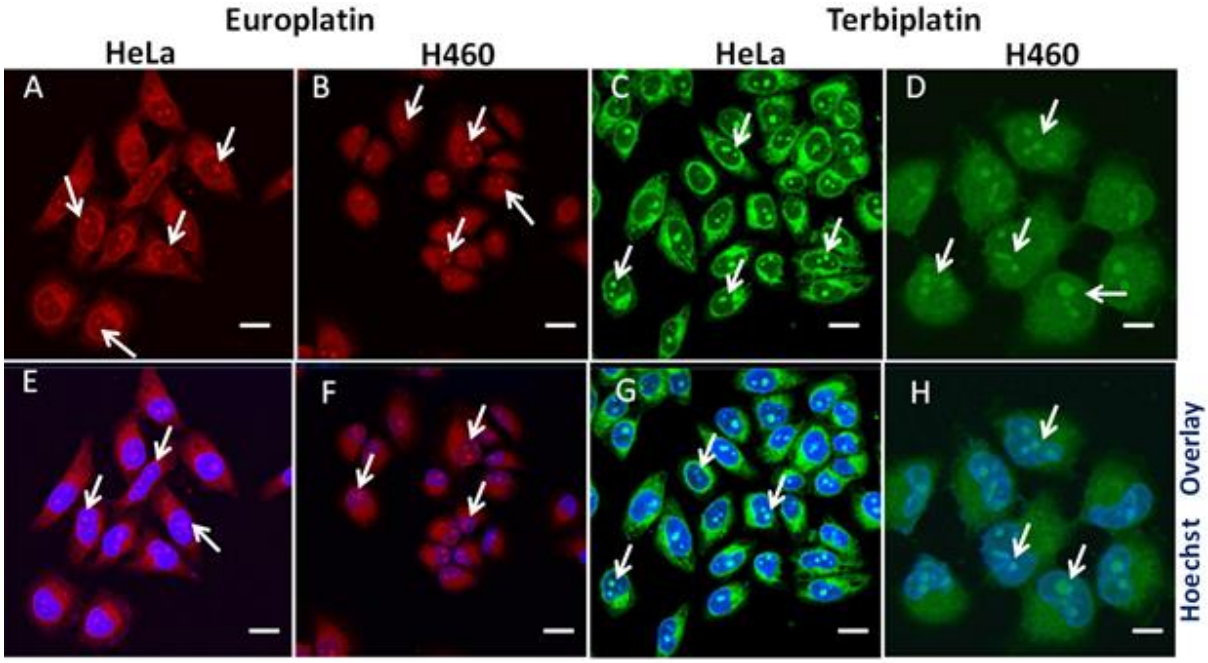


**Figure S16.** Confocal fluorescence microscopic images of the HeLa and H460 cell treated with the europlatin (**1**) **(**A, D**)** and terbiplatin (**2**) **(**G, J**)** (25 $\mu$M) respectively after 4 h of incubation (C, F, I, L) merged images showing nuclear localization of the complex **1** and **2** respectively; Scale bar = 20 $\mu$m. Arrow head indicating the bright red and green spots from nucleoli originated from $Eu^{III}$ and $Tb^{III}$ -based luminescence from complex **1** and **2** inside the nucleli.

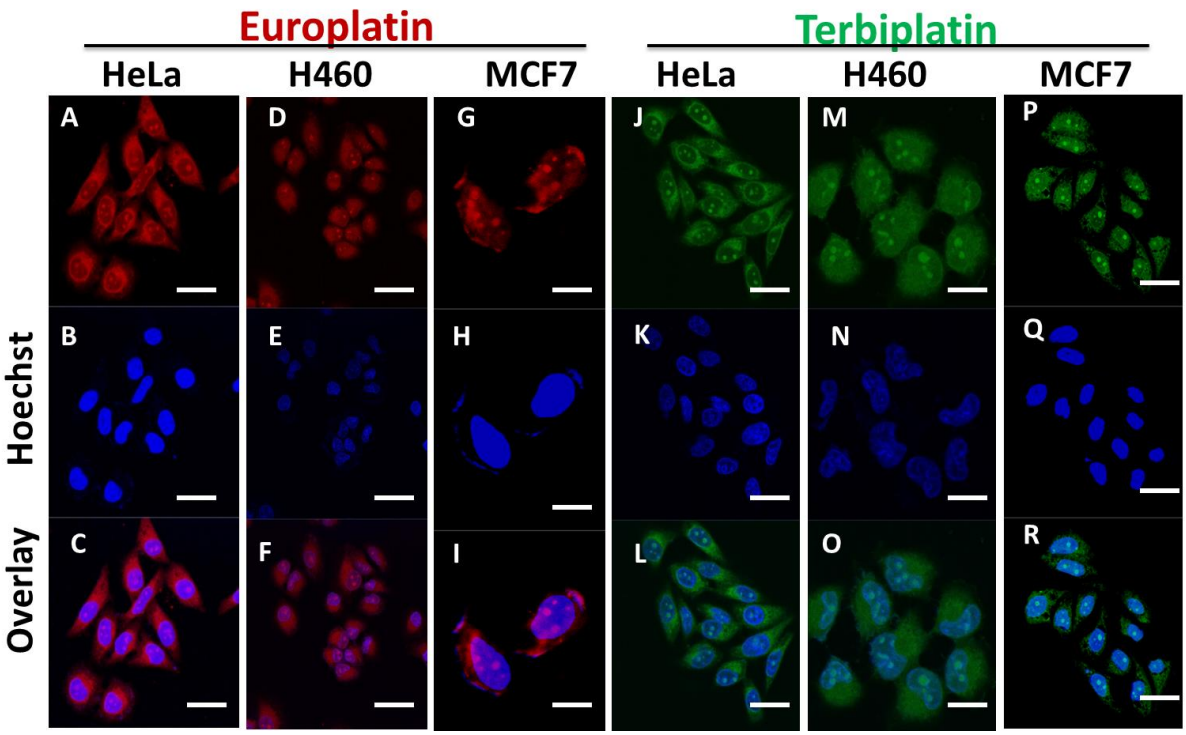


**Fig. S17.** Confocal fluorescence microscopic images of the HeLa, H460 and MCF7 cells showing the intracellular localization profile when treated with 25 $\mu$M of europlatin (**1**) (A, D, G)**,** terbiplatin (**2**) (J, M, P) and Hoechst 33258 dye (5 $\mu$g mL$^{-1}$) (B, E, H, K, N, Q) for staining nuclei; merged images showing nuclear localization of the complexes **1** and **2** respectively (C, F, I, L, O, R); incubation time = 4 h, scale bar = 20 $\mu$m, $\lambda_{ex}$ = 405 nm for complex **1** and 488 nm for complex **2**.

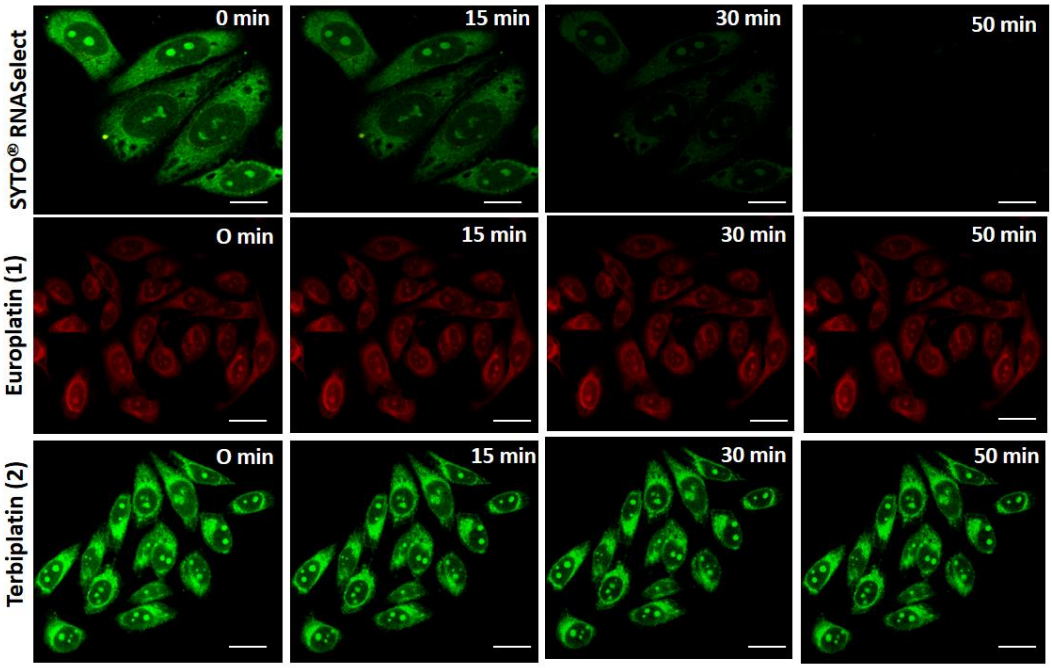


**Fig. S18.** Time-dependent photostability study in HeLa cells with SYTO® RNASelect (top channels), europlatin (**1**) (middle channels) and terbiplatin (**2**) (bottom channels). Scale bar = 20 $\mu$m, $\lambda_{ex}$ = 405 nm for europlatin (**1**) and 488 nm for terbiplatin (**2**) and SYTO® RNASelect.